

## Magnetic field dependence of the London penetration depth in the vortex state of $\text{YBa}_2\text{Cu}_3\text{O}_{6.95}$

J. E. Sonier, R. F. Kiefl, J. H. Brewer, D. A. Bonn, S. R. Dunsiger, W. N. Hardy, Ruixing Liang, W. A. MacFarlane, and T. M. Riseman\*

*TRIUMF, Canadian Institute for Advanced Research and Department of Physics, University of British Columbia, Vancouver, British Columbia, Canada V6T 1Z1*

D. R. Noakes and C. E. Stronach

*Department of Physics, Virginia State University, Petersburg, Virginia 23806*

(Received 19 December 1996)

The magnetic penetration depth in the vortex state of  $\text{YBa}_2\text{Cu}_3\text{O}_{6.95}$  has been measured as a function of temperature  $T$  and magnetic field  $H$  applied along the  $\hat{c}$  axis. The internal field distribution in single crystals was fit assuming a triangular vortex lattice with an average in-plane penetration depth  $\lambda_{ab} = (\lambda_a \lambda_b)^{1/2} = 1155(3)$  Å, extrapolated to  $T=0$  and  $H=0$ ;  $\lambda(H,T)$  increases with both  $T$  and  $H$ . The large  $T$ -independent increase in  $\lambda_{ab}$  with  $H$  is attributed to a strong nonlinear response as a result of the unconventional pairing in the superconducting state. [S0163-1829(97)01717-7]

Measurements of the magnetic penetration depth  $\lambda$  in a superconductor provide important information on the superfluid density and how it changes as a function of temperature, magnetic field and impurities. Recent studies of high- $T_c$  superconductors have focused primarily on the temperature dependence of  $\lambda$ , which is sensitive to the spectrum of low lying excitations and thus the nature of the superconducting state. In particular, microwave cavity measurements in the Meissner state<sup>1</sup> and muon spin rotation ( $\mu\text{SR}$ ) measurements in the vortex state of  $\text{YBa}_2\text{Cu}_3\text{O}_{6.95}$  (Ref. 2) have clearly demonstrated that in the best crystals there is a linear increase of the penetration depth as a function of temperature. This remains one of the strongest pieces of evidence for unconventional pairing in which there are line nodes in the superconducting energy gap function leading to a linear density of states  $\rho(E)$  for low lying excitations.

Much less is known about how  $\lambda$  varies with magnetic field. In the Meissner state of a conventional superconductor one expects a weak quadratic field dependence,

$$\lambda(H,T)/\lambda(0,T) = 1 + \beta_1(T)[H/H_0]^2, \quad (1)$$

where  $H_0$  is a characteristic field on the order of the thermodynamic critical field. Near  $T_c$  this behavior arises from thermodynamic considerations within Ginzburg-Landau (GL) theory<sup>3</sup> and the rapid variation in  $\lambda$  near  $T_c$ . At low temperatures a small quadratic field dependence comes from nonlinear corrections to the London equations<sup>4</sup> due to the fact that the supercurrent density does not scale exactly with the velocity of the superfluid. The essential point is that a supercurrent causes pair breaking, leading to a decrease in the superfluid density as a function of increasing magnetic field or superfluid velocity. In a conventional  $s$ -wave superconductor, where there is an appreciable energy gap over the entire Fermi surface,  $\beta_1(T)$  is much less than 1 at low temperatures and vanishes as the temperature approaches zero.<sup>5</sup>

A much stronger magnetic field dependence of  $\lambda$  is expected for a superconductor with an unconventional pairing state in which there are nodes in the energy gap function.

The qualitative difference is due to the fact that quasiparticles can easily be excited at all temperatures. In the case of  $d_{x^2-y^2}$  pairing, Yip and Sauls<sup>5</sup> have predicted a strong linear field dependence for  $\lambda(H,0)$  in the Meissner state:

$$\lambda(H,T)/\lambda(0,T) = 1 + \beta_2(T)[H/H_0], \quad (2)$$

where  $H_0 = \phi_0 / (\pi^2 \lambda \xi)$ ,  $\xi$  is the coherence length and  $\phi_0 = 2.068 \times 10^{-15}$  T m<sup>2</sup>. Unlike in conventional superconductors, the prefactor  $\beta_2$  remains large at  $T=0$ . Recently, Stojkovic *et al.* have studied this effect at finite temperature and for different pairing schemes.<sup>6</sup> For  $d_{x^2-y^2}$  pairing they predict a crossover temperature  $T^*(H)$  below which  $\lambda(H,T)$  is linear in  $H$  but quadratic in  $T$  and above which  $\lambda(H,T)$  is quadratic in  $H$  and linear in  $T$ . Maeda *et al.*<sup>7</sup> have reported a strong linear  $H$  dependence for  $\lambda$  in the Meissner state of single-crystal  $\text{Bi}_2\text{Sr}_2\text{CaCu}_2\text{O}_y$ , which also shows a quadratic increase of  $\lambda$  with temperature. Early measurements of  $\lambda(H,T)$  in a single crystal of  $\text{YBa}_2\text{Cu}_3\text{O}_{6.95}$  found a large  $H^2$  term<sup>8</sup> but the sample had a reduced  $T_c$ , indicating that there may have been extrinsic effects due to impurities.

We report  $\mu\text{SR}$  measurements of the magnetic field dependence of the effective in-plane penetration depth  $\lambda_{ab} = (\lambda_a \lambda_b)^{1/2}$  in the vortex state of twinned single crystals of  $\text{YBa}_2\text{Cu}_3\text{O}_{6.95}$ . The  $T$  dependence of  $\lambda_{ab}$  in these crystals, which is linear at all magnetic fields considered, agrees within the accuracy of the measurements with microwave cavity results near zero magnetic field.<sup>1</sup> Our most important finding is that  $\lambda_{ab}$  extrapolated to zero temperature increases strongly as a function of magnetic field in the vortex state. We attribute this behavior to a strong nonlinear response as a result of the unconventional pairing.

The measurements reported here were taken on two different  $\text{YBa}_2\text{Cu}_3\text{O}_{6.95}$  samples with identical transition temperatures (93.2 K) and transition widths of less than 0.25 K. The first sample was a mosaic of the same three crystals used in Ref. 2 and the second was a large single crystal measuring  $5 \times 5 \times 0.1$  mm<sup>3</sup>. Details of the crystal growth and characterization may be found elsewhere.<sup>2,9</sup> The  $\mu\text{SR}$  experiments

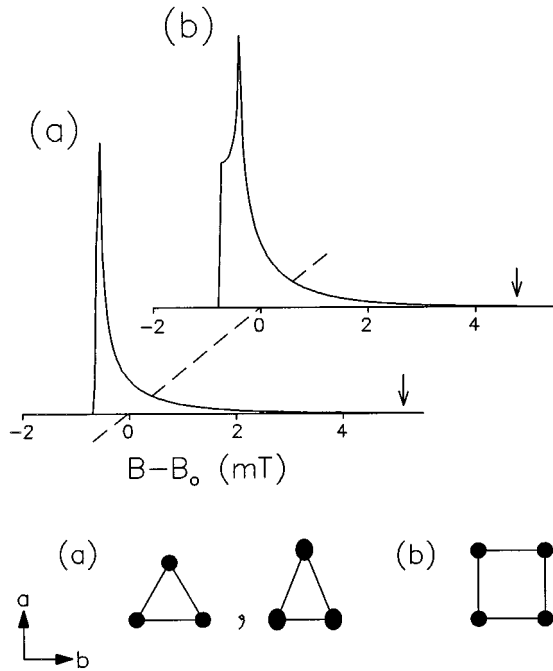


FIG. 1. Magnetic field distributions in the vortex state of a type-II superconductor predicted from a modified London model [see Eq. (3)]. In all cases the external magnetic field is 0.5 T with an average penetration depth perpendicular to the field  $(\lambda_a \lambda_b)^{1/2} = 1217 \text{ \AA}$  and GL parameter  $\kappa = 68$ . The cases shown are (a) a triangular vortex lattice (in which  $\lambda_a/\lambda_b$  need not be equal to 1) and (b) a square lattice in which  $\lambda_a/\lambda_b = 1$ .

were performed on the M15 and M20 surface muon beamlines at TRIUMF using a special low background apparatus designed specifically for studying small crystals.<sup>2,10,11</sup> Except for a few special cases, the measurements were taken after cooling the sample in an external magnetic field applied along the  $\hat{c}$  axis (perpendicular to the  $\text{CuO}_2$  planes) in order to generate the most uniform lattice of vortices.

In a transverse field  $\mu\text{SR}$  experiment one measures the time evolution of the muon polarization vector  $[P_x(t), P_y(t)]$  which precesses about the internal magnetic field. Since the implanted muons stop randomly over regions large compared with the length scale of the flux lattice, the  $\mu\text{SR}$  frequency spectrum is proportional to the magnetic field distribution in the sample,  $n(B)$ . For hard type-II superconductors in the field region being considered here ( $H_{c1} \leq H \leq H_{c2}$ ),  $n(B)$  is determined primarily by the London penetration depth and the geometry of the vortex lattice. At low temperatures and low magnetic fields, changes in the coherence length  $\xi$  (or equivalently the GL parameter  $\kappa = \lambda/\xi$ ) only produces changes in the high-field tail of  $n(B)$  corresponding to the region of the vortex cores.

The  $\mu\text{SR}$  time spectra (see, for example, Fig. 1 in Ref. 2) were fit in a manner outlined therein. Theoretical field distributions were generated using the London model, modified to take into account the finite coherence length.<sup>12</sup> For a perfect vortex lattice the local field at any point in the  $\hat{a}\text{-}\hat{b}$  plane is then given by

$$B(\mathbf{r}) = B_0 \sum_{\mathbf{K}} \frac{e^{-i\mathbf{K} \cdot \mathbf{r}} e^{-K^2 \lambda_{ab}^2 / 2(1-b)\kappa^2}}{1 + K^2 \lambda_{ab}^2 / (1-b)}, \quad (3)$$

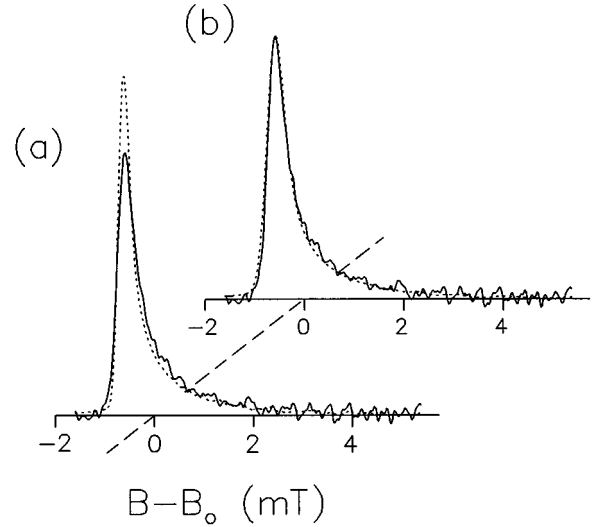


FIG. 2. The solid curve in both (a) and (b) is the same Fourier transform of the muon spin precession signal in single-crystal  $\text{YBa}_2\text{Cu}_3\text{O}_{6.95}$  cooled to 4.25 K in an external field of 0.5 T applied along the  $\hat{c}$  axis (see text). The dashed curve in (b) shows the best fit to the stretched triangular lattice, whose field distribution is shown in Fig. 1(a), including a Gaussian broadening due to a 3% disorder in the flux lattice. The dashed curve in (a) is the Fourier transform of the muon polarization generated from the field distribution in Fig. 1(a) without any Gaussian broadening.

where  $B_0$  is the average magnetic field,  $b = B_0/B_{c2}$ ,  $\lambda_{ab} = (\lambda_a \lambda_b)^{1/2}$  and  $\kappa$  is fixed at a value 68 determined previously.<sup>2,13</sup> The summation is over all reciprocal lattice vectors of a triangular vortex lattice. This is the vortex geometry which minimizes the free energy for a conventional anisotropic superconductor.<sup>14-16</sup> Figure 1(a) shows the theoretical field distribution for a triangular lattice. For comparison we present the field distribution pertaining to a square vortex lattice in Fig. 1(b), normalized to the same peak height. For a conventional superconductor with the external magnetic field parallel to the crystallographic  $\hat{c}$  axis, anisotropy in the  $\hat{a}\text{-}\hat{b}$  plane results in a stretched-triangular vortex lattice in which the primitive basis vectors scale with the mass anisotropy. However, the field distribution for the triangular lattice is independent of the anisotropy parameter  $\gamma^{-2} = \lambda_a/\lambda_b$ , because any change in  $\gamma^{-2}$  is compensated for by rescaling the coordinates in Eq. (3). Far infrared reflectance measurements in zero field have found that  $\gamma^{-2} = 1.47(14)$  and  $\lambda_{ab} = 1325(60) \text{ \AA}$ , averaged over two samples similar to those used in the present study.<sup>17</sup>

The solid curve in each of Figs. 2(a) and 2(b) is the finite Fourier transform of the time spectrum from the large single crystal at  $T = 4.25 \text{ K}$ . For illustrative purposes, the spectrum shown in Fig. 2 was taken by first cooling in a magnetic field of 0.5 T and then reducing the field by 5 mT. This small shift in field has no detectable effect on the field distribution in the sample at low temperatures where the vortex lattice is held rigid by pinning forces. However, such a shift moves a small background line to lower frequencies so that the field distribution in the sample can be viewed without obstruction. The magnitude of this background signal corresponds to about 5% of the sample signal and is due to a small inefficiency in

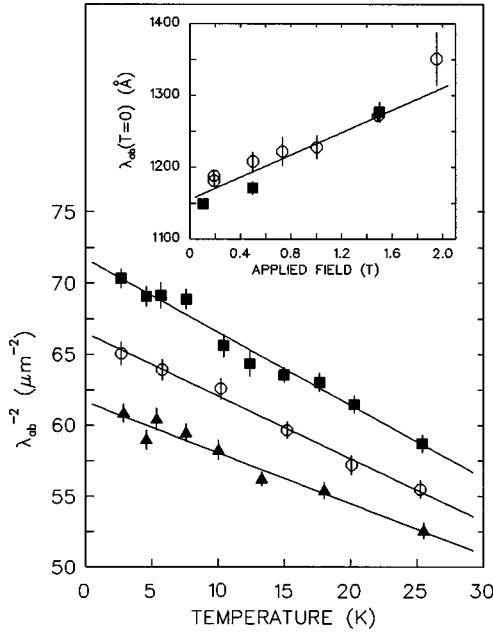


FIG. 3. The temperature dependence of  $\lambda_{ab}^{-2}(T, H)$  in  $\text{YBa}_2\text{Cu}_3\text{O}_{6.95}$  for applied magnetic fields of 0.2 (solid squares), 1.0 (circles), and 1.5 T (solid triangles). The inset shows the field dependence of  $\lambda_{ab}$  extrapolated to  $T=0$  as a function of applied magnetic field. The data for the three-crystal mosaic (Ref. 18) are shown as open circles whereas solid squares are for the large single crystal.

the background suppression system. The dashed curve in Fig. 2(b) is a Fourier transform of the simulated muon polarization function which best fits the data. The values of  $\chi^2$  were typically 220 for 150 degrees of freedom.

In order to obtain fits of the quality shown in Fig. 2(b) it was necessary to allow for a Gaussian broadening of the internal field distribution, which is likely due to a small amount of random disorder in the flux lattice (about 3% of the lattice constant in this case).<sup>2</sup> In Fig. 2(a) the same data are compared with a theoretical transform generated with the same fitting parameters but without the additional Gaussian broadening. Comparison of the two dashed curves in Fig. 2 shows the high sensitivity of the line shape to even a small amount of disorder in the flux lattice. The dashed line in Fig. 2(b) represents the best fit to the data. It is clear that the internal field distribution is close to that predicted for a stretched triangular lattice in an anisotropic conventional superconductor. Comparison of the dashed curve in Fig. 2(a) with the corresponding field distribution in Fig. 1(a) shows how the finite Fourier transformation smears the sharp features in  $n(B)$ . Consequently, one cannot readily distinguish vortex lattice structures with similar internal field distributions by simply inspecting the finite Fourier transforms of the corresponding muon spin precession signals. This is one of the reasons why the actual fitting is done in the time domain.

Figure 3 shows the low temperature behavior of  $\lambda_{ab}^{-2}$  for three of the magnetic fields considered. Excellent fits were obtained to a linear relation:

$$\lambda^{-2}(T) = \lambda^{-2}(0)[1 - \alpha T]. \quad (4)$$

The linear term is essentially independent of magnetic field to within the systematic uncertainties. Also the linear coefficient  $\alpha$  agrees well with microwave cavity measurements of  $d\lambda/dT$  at low temperatures in zero magnetic field<sup>1</sup> after  $d\lambda/dT$  has been converted into  $d\lambda^{-2}/dT$  using our absolute value of  $\lambda$ .

The inset of Fig. 3 shows the field dependence of  $\lambda_{ab}$  extrapolated to  $T=0$ . The error bars represent the systematic uncertainties in  $\lambda(T=0)$  that we estimate by fitting random subsets of the  $\lambda(T)$  data for each magnetic field. The solid line is a fit of the entire data set to a power law:

$$\lambda_{ab}(H, T=0) = \lambda_{ab}(0, 0) + \beta H^p, \quad (5)$$

where  $\lambda_{ab}(0, 0) = 1155(3) \text{ \AA}$ ,  $\beta = 78(3) \text{ \AA/T}$  and  $p = 1.0(1)$ . Since the data in Fig. 3 are only a small subset of the entire field range below  $H_{c2}$ , one cannot conclude that the full field dependence of the penetration depth is linear. We stress that the qualitative features in Fig. 3 are not sensitive to the precise choice of the vortex lattice structure. For instance, although the square lattice of Fig. 1(b) yields much worse fits to the data, the field dependence of  $\lambda_{ab}$  remains unchanged.

So far there is no detailed theory for the effects of a nonlinear supercurrent response in the vortex state with which to compare our results. However, one would expect the change in the penetration depth to scale roughly with the average supercurrent density. In the Meissner state the supercurrent density  $J$  increases almost linearly as function of  $H$ . However, in the vortex state the average supercurrent density  $\langle J \rangle = \langle |\nabla \times \mathbf{B}(\mathbf{r})| \rangle / \mu_0$  scales roughly as  $H^{0.41}$  in the field range of our investigation, for  $\mathbf{B}(\mathbf{r})$  defined by the modified London model of Eq. (3).<sup>19</sup> Within this model, a linear increase in  $\lambda$  with magnetic field in the vortex state would correspond to  $\lambda \propto \langle J \rangle^{2.4(7)}$ . In the Meissner state this would translate to an  $H^{2.4(7)}$  dependence. However, one must be very careful in making such a comparison, as there are several qualitative differences between the vortex and Meissner states. In particular the field and current distributions are very different. Also the peak and average current densities in the vortex state are much higher than in the Meissner state. In the vortex state at 1 T the average current density  $\langle J \rangle = 4.2 \times 10^7 \text{ A cm}^{-2}$  whereas in the Meissner state at  $H = 10 \text{ mT}$  at a distance  $\lambda = 1200 \text{ \AA}$  from the surface,  $J$  is 10 times smaller. It is clear that a detailed comparison with theory will require an extension of the theory for nonlinear effects in the vortex state.

We note that there have been attempts to explain the magnetic field dependence of the  $\mu\text{SR}$  linewidth in some of the earlier studies in terms of vortex fluctuations.<sup>20</sup> However, such corrections to the penetration depth would be small below 30 K where we observe a large field dependence. In fact at high temperatures such as 80 K, where vortex fluctuations would be largest, there was no detectable field dependence.

It is possible that the unit cell of the vortex lattice in  $\text{YBa}_2\text{Cu}_3\text{O}_{7-\delta}$  is something other than triangular. Recent STM measurements on single crystals<sup>21</sup> support an earlier neutron scattering study<sup>22</sup> which determined that the vortex lattice in  $\text{YBa}_2\text{Cu}_3\text{O}_{7-\delta}$  is oblique, with nearly equal primitive vectors forming an angle of approximately  $75^\circ$ . Both

experiments also suggest that one of the primitive vectors is oriented at an angle of  $45^\circ$  with respect to either the  $\hat{a}$  or  $\hat{b}$  axis. No current theory, however, provides an intrinsic mechanism which gives the orientation of the vortex lattice with respect to the crystallographic axis seen in STM and neutron scattering experiments. An oblique lattice may exist in orthorhombic  $\text{YBa}_2\text{Cu}_3\text{O}_{7-\delta}$  if the expected hexagonal vortex lattice aligns itself with twin boundaries, as argued by Walker and Timusk.<sup>23</sup> Hence, the vortex lattice may very well be a triangular or stretched-triangular lattice in a sparsely twinned sample of  $\text{YBa}_2\text{Cu}_3\text{O}_{6.95}$ . Vortex-imaging experiments on untwinned crystals are needed to resolve this issue. Another possibility is that upon field cooling our sample, the vortex structure just below  $T_c$  (which is predicted to be triangular for a  $d$ -wave superconductor in the context of GL theory<sup>24</sup>) becomes strongly pinned and maintains its geometry down to low temperature. We have already demonstrated the strong pinning of the vortex lattice in our samples at low temperatures (see discussion for Fig. 2). The lattice remains pinned upon warming the sample, up to

approximately  $0.8T_c$ . We stress that any changes in the vortex structure assumed in our fits would only alter the absolute values of  $\lambda_{ab}$  and would have a negligible effect on the qualitative  $T$  and  $H$  dependences of  $\lambda_{ab}$ .

In conclusion, we observe a strong  $H$  dependence at low  $T$  for the in-plane penetration depth in the vortex state of single crystals of  $\text{YBa}_2\text{Cu}_3\text{O}_{6.95}$ . In addition, the linear  $T$  dependence which has been observed previously is found to be independent of  $H$  in the field range studied. The strong  $T$  and  $H$  behavior of  $\lambda(H, T)$  are attributed to the unconventional pairing state.

We would like to thank Ian Affleck, John Berlinsky, Catherine Kallin, Marcel Franz, and Mohammad Sharifzadeh for many helpful discussions and Syd Kreitzman, Keith Hoyle, Curtis Ballard, and Mel Good for technical assistance. This work is supported by the Natural Sciences and Engineering Research Council of Canada and by the U.S. Department of Energy through Grant No. DE-FG05-88ER45353.

\*Present address: Department of Physics, University of Indiana, Bloomington, IN 47406.

<sup>1</sup>W.N. Hardy, D.A. Bonn, D.C. Morgan, R. Liang, and Kuan Zhang, *Phys. Rev. Lett.* **70**, 3999 (1993).

<sup>2</sup>J.E. Sonier *et al.*, *Phys. Rev. Lett.* **72**, 744 (1994).

<sup>3</sup>V.L. Ginzburg and L.D. Landau, *Zh. Éksp. Teor. Fiz.* **20**, 1064 (1950).

<sup>4</sup>J. Bardeen, *Phys. Rev.* **94**, 554 (1954).

<sup>5</sup>S.K. Yip and J.A. Sauls, *Phys. Rev. Lett.* **69**, 2264 (1992).

<sup>6</sup>B.P. Stojković and O.T. Valls, *Phys. Rev. B* **51**, 6049 (1995).

<sup>7</sup>A. Maeda *et al.*, *Phys. Rev. Lett.* **74**, 1202 (1995).

<sup>8</sup>S. Sridhar, Dong-Ho Wu, and W. Kennedy, *Phys. Rev. Lett.* **63**, 1873 (1989).

<sup>9</sup>R. Liang *et al.*, *Physica C* **195**, 51 (1992).

<sup>10</sup>J.W. Schneider *et al.*, *Phys. Rev. Lett.* **71**, 557 (1993).

<sup>11</sup>J.E. Sonier, M.Sc. thesis, University of British Columbia, 1994.

<sup>12</sup>E.H. Brandt, *J. Low Temp. Phys.* **26**, 709 (1977); **73**, 355 (1988); E.H. Brandt, *Phys. Rev. B* **37**, 2349 (1988).

<sup>13</sup>T.M. Riseman *et al.*, *Phys. Rev. B* **52**, 10 569 (1995).

<sup>14</sup>L.J. Campbell, M.M. Doria, and V.G. Kogan, *Phys. Rev. B* **38**, 2439 (1988).

<sup>15</sup>S.L. Thiemann, Z. Radovic, and V.G. Kogan, *Phys. Rev. B* **39**, 11 406 (1989).

<sup>16</sup>L.L. Daemen, L.J. Campbell, and V.G. Kogan, *Phys. Rev. B* **46**, 3631 (1992).

<sup>17</sup>D.N. Basov *et al.*, *Phys. Rev. Lett.* **74**, 598 (1995).

<sup>18</sup>The values of  $\lambda_{ab}(0)$  at 0.5 and 1.5 T are slightly different than those which appear in Ref. 2. The difference is due to a premature cutoff of the summation in Eq. (3) used in the previous analysis.

<sup>19</sup>The weaker field dependence in the vortex state originates from the fact that the peak supercurrent density which occurs just outside the cores, is almost field independent. The increase in  $\langle J \rangle$  with magnetic field results from the increase in the vortex density.

<sup>20</sup>Y. Song, *Physica C* **241**, 187 (1995).

<sup>21</sup>I. Maggio-Aprile, Ch. Renner, A. Erb, E. Walker, and O. Fischer, *Phys. Rev. Lett.* **75**, 2754 (1995).

<sup>22</sup>B. Keimer *et al.*, *Phys. Rev. Lett.* **73**, 3459 (1994).

<sup>23</sup>M.B. Walker and T. Timusk, *Phys. Rev. B* **52**, 97 (1995).

<sup>24</sup>Ji-Hai Xu, Y. Ren, and C. S. Ting, *Int. J. Mod. Phys. B* **10**, 2699 (1996).